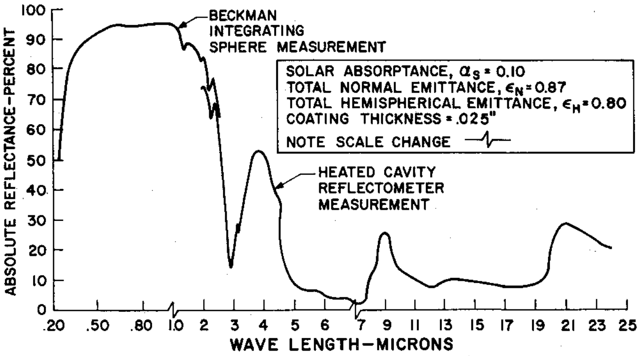

Fig. 1 Spectral reflectance of experimental coating

Table 1 Optimum coating design

Solar wavelength intervals, μ	Particle distribution, %	Particle size diam, μ
0.20 to 0.47	18	0.38
0.47 to 0.60	28	0.53
0.60 to 0.93	30	0.75
0.93 to 1.30	16	1.09
1.30 to 2.60	8	1.90

Under subcontract from the General Electric Company, Re-Entry Systems Department, Corning Glass Works in conjunction with Dow-Corning† formulated a paint whose optical properties approach those of the Corning #7941, multiform fused silica. The pigment consists of fine particles of ultrapure fused silica, and the paint vehicle is an experimental silicone varnish that evaporates at elevated temperature leaving a matrix of fine particles of fused silica with good adhesion. Figure 1 illustrates the results of optical reflection measurements performed on the experimental coating for a coating thickness of 25 mils. Reduction of the near-normal spectral reflection data yields a solar absorptance of 0.10 and a total hemispherical emittance of 0.80. The coating formulation presently is undergoing ultraviolet, vacuum exposure, and it is anticipated that the coating will be very stable since its singular ingredient, i.e., ultrapure fused silica, is transparent to the ultraviolet spectrum above 2000 Å. The Corning grade #7940 fused silica is also extremely resistant to particle radiation.

It is speculated that further optimization of the experimental coating (lower absorptance) may be achieved by adjusting the particle size and particle size distribution of the fused silica. The following equation defines the optimum particle size for maximum scattering of wavelength λ:[1]

$$d = (0.90\lambda/n_0\pi)[(m^2 + 2)/(m^2 - 1)]$$

where λ is the wavelength to be scattered in microns, n_0 is the index of refraction of the vehicle, m is the ratio of the index of refraction of the pigment of the vehicle, and d defines the optical particle size diameter in microns. The particle distribution would be determined by the spectrum of radiation to be scattered. Table 1 lists a possible particle size and particle size distribution for optimum reflection of solar illumination.

In addition to the spacecraft application, the coating has been suggested to the National Bureau of Standards as a possible secondary optical standard and also may be suitable as an interior coating for integrating spheres.

† F. Bickford of the Corning Research Laboratory directed efforts that led to paint development.

[1] Tomkins, M. and Tomkins, H., "The design of heat-reflective paints," J. Oil Colour Chemist Assoc. **41**, 98–108 (January 1958).

Measure of Satellite Dispersion

E. D. Callender* and J. B. Day†

Philco Corporation, Palo Alto, Calif.

A measure of symmetry is found for a set of coplanar vehicles. This measure can be applied to the case where the vehicles are launched simultaneously from a carrier vehicle. For a given period of time, an optimal burst configuration can be determined. However, as the period of time increases, the difference in the measure of an optimal and nonoptimal burst configuration approaches zero.

In the study of orbital configurations for satellites used in communications systems, it is highly desirable to have the vehicles in symmetric position. Unfortunately, because of launch considerations and perturbing influences, it is virtually impossible to maintain symmetric positioning. In particular, if a set of coplanar vehicles results from the subvehicles being launched simultaneously from a carrier vehicle, the configuration is subject to continual variation. Two problems arise. The first is to find some measure of symmetry, and the second is to determine optimal launch distribution of the subvehicles from the carrier vehicle. It is natural to take as a measure of symmetry the variations from the optimal symmetric state.

A necessary and subject condition that a symmetric distribution exists is that

$$\sum_{j=1}^{K} \begin{pmatrix}\sin\\ \cos\end{pmatrix} M\alpha_j = 0$$

for a proper range of M, where α_j is the sum of the true anomaly and argument of perigee for the jth vehicle. This is because the symmetric distribution of K vehicles has an analogy in a display of the K roots of unity on the complex plane.

Proof: Given

$$\sum_{j=1}^{K} \begin{pmatrix}\sin\\ \cos\end{pmatrix} M\alpha_j = 0 \qquad M = 1, 2, 3, \ldots$$

consider

$$\prod_{=1}^{K} (X - e^{i\alpha_j}) = 0$$

Then the expansion

$$X^K + a_1 X^{K-1} + a_2 X^{K-2} + \ldots + a_{K-1} X^1 + a_K = 0$$

has as coefficients

$$a_1 = -\sum_{j=1}^{K} e^{i\alpha_j} = 0$$

if

$$\sum_{j=1}^{K} e^{i\alpha_j} = 0$$

$$a_2 = +\sum_{\substack{1\\ j_1 < j_2}}^{K} e^{i(\alpha_{j_1} + \alpha_{j_2})} = -\frac{1}{2}\sum_{j=1}^{K} e^{i2\alpha_j} = 0$$

Received by ARS August 22, 1962; revision received January 2, 1963.

* Manager, Problem Analysis Section, Mathematical Analysis Department, Western Development Laboratories.

† Senior Engineer, Problem Analysis Section, Western Development Laboratories.

if

$$\sum_{j=1}^{K} e^{i\alpha_j} = 0 \qquad \sum_{j=1}^{K} e^{i2\alpha_j} = 0$$

$$a_3 = -\sum_{\substack{1 \\ j_1 < j_2 < j_3}}^{K} e^{i(\alpha_{j_1}+\alpha_{j_2}+\alpha_{j_3})} = -\frac{1}{3}\sum_{j=1}^{K} e^{i3\alpha_j} = 0$$

if

$$\sum_{j=1}^{K} e^{i\alpha_j} = 0 \qquad \sum_{j=1}^{K} e^{i2\alpha_j} = 0 \qquad \sum_{j=1}^{K} e^{i3\alpha_j} = 0$$

.
.
.

$$a_{K-3} = (-1)^{K-3}\sum_{1}^{K} e^{i(\alpha_{j_1}+\alpha_{j_2}+\ldots+\alpha_{j_{K-3}})} =$$

$$a_K(-1)^{K-3}\frac{1}{3}\sum_{\substack{j=1 \\ < j_2 < \ldots < j_{K-3}}}^{K} e^{-i3\alpha_j} = 0$$

if $a_3 = 0$,

$$a_{K-2} = (-1)^{K-2}\sum_{1}^{K} e^{i(\alpha_{j_1}+\alpha_{j_2}+\ldots+\alpha_{j_{K-2}})} =$$

$$a_K(-1)^{K-2}\left(-\frac{1}{2}\right)\sum_{\substack{j=1 \\ j_1 < j_2 < \ldots < j_{K-2}}}^{K} e^{-i2\alpha_j} = 0$$

if $a_2 = 0$,

$$a_{K-1} = (-1)^{K-1}\sum_{1}^{K} e^{i(\alpha_{j_1}+\alpha_{j_2}+\ldots+\alpha_{j_{K-1}})} =$$

$$a_K(-1)^{K-1}\sum_{\substack{j=1 \\ j_1 < j_2 < \ldots < j_{K-1}}}^{K} e^{-i\alpha_j} = 0$$

if $a_1 = 0$,

$$a_K = (-1)^K \sum_{\substack{1 \\ j_1 < j_2 < \ldots < j_K}}^{K} e^{i(\alpha_{j_1}+\alpha_{j_2}+\ldots+\alpha_{j_K})}$$

Note that conditions for $a_n = 0 \rightarrow a_{K-n} = 0$. Hence, the number of conditions is $+K/2+$ (the desired range for M).

Now, for a set of vehicles in circular orbits, considering any vehicle as a reference with mean angular rate n_0, the position of another vehicle with respect to the reference is, at time t,

$$\alpha_i = (n_0 + \Delta n_i)\, t$$

where Δn_i is the difference in mean angular rate. Letting the reference vehicle position $n_0 t = 0$, one has $\alpha_i = \Delta_{n_i} t$.

One possible measure of lack of symmetry then can be expressed as

$$Q = \frac{1}{T_2 - T_1}\int_{T_1}^{T_2}\left\{\left[\sum_{1}^{K-1} \sin\Delta n_i t\right]^2 + \left[1 + \sum_{1}^{K-1}\cos\Delta n_i t\right]^2 + \ldots + \left[\sum_{1}^{K-1}\sin\left[\frac{K}{2}\right]\Delta n_i t\right]^2 + \left[1 + \sum_{1}^{K-1}\cos\left[\frac{K}{2}\right]\Delta n_i t\right]^2\right\} dt$$

over the time interval T_1 to T_2. To facilitate presentation, suppose $K = 5$; then,

$$Q = \frac{1}{T_2 - T_1}\int_{T_1}^{T_2}\left\{\left[\sum_{1}^{4}\sin\Delta n_i t\right]^2 + \left[1 + \sum_{1}^{4}\cos\Delta n_i t\right]^2 + \left[\sum_{1}^{4}\sin 2\Delta n_i t\right]^2 + \left[1 + \sum_{1}^{4}\cos 2\Delta n_i t\right]^2\right\} dt$$

and

$$Q = 10 + \frac{2}{T_2 - T_1}\left[\sum_{\substack{1 \\ i>j}}^{4}\frac{\sin(\Delta n_i - \Delta n_j)T_2}{\Delta n_i - \Delta n_j} - \sum_{\substack{1 \\ i>j}}^{4}\frac{\sin(\Delta n_i - \Delta n_j)T_1}{\Delta n_i - \Delta n_j} + \frac{1}{2}\sum_{\substack{1 \\ i>j}}^{4}\frac{\sin 2(\Delta n_i - \Delta n_j)T_2}{\Delta n_i - \Delta n_j} - \frac{1}{2}\sum_{\substack{1 \\ i>j}}^{4}\frac{\sin 2(\Delta n_i - \Delta n_j)T_1}{\Delta n_i - \Delta n_j} + \sum_{1}^{4}\frac{\sin\Delta n_i T_2}{\Delta n_i} - \sum_{1}^{4}\frac{\sin\Delta n_i T_1}{\Delta n_i} + \frac{1}{2}\sum_{1}^{4}\frac{\sin 2\Delta n_i T_2}{\Delta n_i} - \frac{1}{2}\sum_{1}^{4}\frac{\sin 2\Delta n_i T_1}{\Delta n_i}\right]$$

Although the foregoing expression would make a rather tedious hand calculation, it is a relatively simple task for a computer. As an illustration, the Δn_i arising from the forementioned simultaneous "launch" situation are subject to certain conditions. For purposes of the study that evolved the need for a measure of dispersion, it was assumed that the carrier vehicle was in a circular orbit of about 5000-naut miles altitude and the subvehicle "burst-off" velocities in the neighborhood of 200 fps. These assumptions allow the use of

$$P = 3\,P(a/\mu)^{1/2}\Delta v \cos\alpha \cos\beta$$

which is an approximation of the change in period of a launched subvehicle, where

P = period of carrier vehicle
Δv = "burst-off" velocity of subvehicle
α = azimuth angle of subvehicle
β = flight path angle of subvehicle
a = radial distance of carrier vehicle
μ = universal gravitation constant

Then

$$n_i = \frac{n}{1 + 3(a/\mu)^{1/2}\Delta v_i \cos\alpha_i \cos\beta_i}$$

where

n_i = mean angular rates of subvehicles
n = $(\mu/a^3)^{1/2}$, the mean angular rate of the carrier vehicle

Then the Δn_i are simply the differences in mean angular rates with respect to an arbitrarily chosen reference vehicle, $\Delta n_i = n_0 - n_i$. The admission of more general systems will require a more stringent evaluation of the Δn_i but will not affect the Q function in any other fashion.

Comment

Excluding cases where either $\Delta n_i = 0$ or $\Delta n_i - \Delta n_j = 0$ (these occurrences imply theoretic continual coincidence), note that $Q \rightarrow 2K$ when $T_2 - T_1 \rightarrow \infty$ independent of the choice of "launch" parameters; however, for discrete time intervals, this Q suffices to provide a reasonable comparison of the respective suitabilities of "launch" parameter choices.

Table 1 Comparative results

Time interval, days	Measured Q	Initial set of Δn_i	Local minimum Q	Optimal set of Δn_i
2 to 16	9.0209	0.5340	6.4260	0.7402
		1.0486		1.4924
		1.5449		1.8387
		2.0239		2.1739
2 to 32	9.1496	0.5340	8.1946	0.5590
		1.0486		1.1236
		1.5449		1.8949
		2.0239		2.0552
2 to 182	9.8488	0.5340	9.6071	0.6340
		1.0486		1.1486
		1.5449		1.2449
		2.0239		1.6177
2 to 367	9.9967	0.5340	9.8012	0.0840
		1.0486		0.6486
		1.5449		1.1195
		2.0239		1.7239

Since the optimal, but unattainable, Q would be zero (the case of rigid symmetry), a subsequent analysis of the behavior of Q as a function of "launch" parameters and time interval was performed. Using a numerical minimization technique, a local minimum Q was determined by finding the optimal Δn_i for a given $T_2 - T_1$ (see Table 1). It was found that, as the time interval was decreased, the local minimum Q diminished, and a distinct set of optimal Δn_i was generated for each $T_2 - T_1$. When $T_2 - T_1$ was increased to one year, the improvement in Q by minimization was neglible. Hence, any choice of "launch" parameters that insure significant differences in mean angular rate will provide acceptable dispersion over long periods of time.

Rarefied Viscous Flow Near a Sharp Leading Edge

Edgar Bendor*
Republic Aviation Corporation, Farmingdale, N. Y.

Nomenclature

M = freestream Mach number
Re = Reynolds number
s = h_w/H_∞
t = $U_\infty^2/2H_\infty$
β = shock inclination
λ = $\gamma C\mu_w U_\infty/(\gamma+1)(\gamma-1)h_w\rho_\infty$
ξ = $(\gamma+1)Re/\gamma t M^2$
χ = $M^3/(Re)^{1/2}$

In the rarefied flow over a sharp edged plate there arises a so-called "viscous layer" regime, in which the strong pressure interaction theories are no longer applicable, but the degree of rarefaction is not yet such that slip and temperature jump need be taken into account. For a cold wall, the regime in question occurs for values of the viscous interaction parameter χ of the order of the square of the freestream Mach number. Neglecting the free molecule and slip regions in the immediate vicinity of the leading edge, the viscous layer is bounded by a (thin) shock wave, originating at the leading edge, behind which the entire flow field is viscous.

Received by ARS October 29, 1962; revision received February 18, 1963.

* Specialist Engineer, Applied Research and Development Division.

Such a model has been treated by Oguchi,[1] using the boundary layer equations, with the assumption that the curvature of the shock wave is zero at the leading edge. Having shown that shear stress and heat conduction are predominant at the leading edge, he simply equates these terms to zero. The basic (vanishing Reynolds number) solution so obtained is modified later to include terms of the next order, but with the downstream coordinate treated as a parameter rather than as an independent variable.

It is shown here that Oguchi's solution may be regarded as the zeroth term of a series solution of the full boundary layer equations in powers of the variable $\xi = [2(\gamma+1)H_\infty/\gamma U_\infty^2](Re/M^2)$ of which the first three terms are derived. The shock angle at the leading edge is found to be $\beta = [(\gamma+1)(\gamma-1)/12\gamma]^{1/2}$ for a cold wall. The validity of the boundary layer approximation in a region with this apex angle is open to question (e.g., Hayes and Probstein[2]). It is apparent, however, that a solution cannot be obtained easily to more general equations, and the fact that the pressure at the leading edge is found to be in good agreement with experiment provides some justification for the following procedure.

If the boundary layer equations for unit Prandtl number are transformed with

$$\eta = \left(\frac{U_\infty}{2x}\right)^{1/2} \int_0^y \rho dy \tag{1}$$

$$f = \int_0^\eta \left(\frac{u}{U_\infty}\right) d\eta \qquad \Theta = \frac{H - h_w}{H_\infty - h_w} \tag{2}$$

then the momentum and energy equations are

$$\frac{\partial}{\partial\eta}\left(\rho\mu\frac{\partial^2 f}{\partial\eta^2}\right) + f\frac{\partial^2 f}{\partial\eta^2} = 2x\left[\left(\frac{\partial f}{\partial\eta}\frac{\partial^2 f}{\partial x\partial\eta}\right) - \left(\frac{\partial f}{\partial x}\frac{\partial^2 f}{\partial\eta^2}\right)\right] + \frac{2x}{\rho U_\infty^2}\frac{dp}{dx} \tag{3}$$

$$\frac{\partial}{\partial\eta}\left(\rho\mu\frac{\partial\Theta}{\partial\eta}\right) + f\frac{\partial\Theta}{\partial\eta} = 2x\left[\left(\frac{\partial f}{\partial\eta}\frac{\partial\Theta}{\partial x}\right) - \left(\frac{\partial f}{\partial x}\frac{\partial\Theta}{\partial\eta}\right)\right] \tag{4}$$

Neglecting the quantity $(U_\infty - u_s) \sim U_\infty O(\beta^2)$, the boundary conditions are

$$\eta = 0 \qquad f = \partial f/\partial\eta = \Theta = 0$$
$$\eta = \eta_s \qquad \partial f/\partial\eta = \Theta = 1 \tag{5†}$$

Continuity requires that

$$\rho_\infty U_\infty y_s = \psi_s = (2U_\infty x)^{1/2} f(x,\eta_s) \tag{6}$$

But from Eq. (1)

$$y_s = \left(\frac{2x}{U_\infty}\right)^{1/2} \int_0^{\eta s} \frac{1}{\rho} d\eta \tag{7}$$

and for an ideal gas

$$1/\rho \approx [(\gamma-1)H_\infty/\gamma p][(1-s)\Theta + s - t(\partial f/\partial\eta)^2] \tag{8}$$

Substituting Eqs. (7) and (8), the continuity condition (6) becomes

$$\left[(\gamma-1)\frac{\rho_\infty H_\infty}{\gamma}\right]\int_0^{\eta_s}\left[(1-s)\Theta + s - t\left(\frac{\partial f}{\partial\eta}\right)^2\right] \times d\eta = p(x)f(x,\eta_s) \tag{9}$$

The outer boundary conditions, which are satisfied at the shock rather than at infinity, suggest transformation to the variable $\eta/\eta_s(x)$. Further, since the shear stress is known to become predominant for vanishing Reynolds number, one may expect the leading term in an expansion of $u(x,\eta)$ to be

† Subscript s refers to conditions just behind the shock wave.